CrossMark

ORIGINAL

Mixed mode fracture behavior of welded wood joints investigated with the Arcan test

Martin Rhême[1] · John Botsis[2] · Joël Cugnoni[2] ·
Parviz Navi[1]

Abstract Friction welding of wood is an assembly method that is still under investigation and development. A possible application for welded wood joints is the fabrication of multi-layered panels (i.e., cross-laminated panels). In an effort to model the behavior of such products, work is needed to characterize the mechanical strength and fracture properties of welded joints produced with parallel and cross-grain orientations. The present work addresses combined experimental and numerical investigations into the strength and fracture characterization of welded wood joints. The Arcan test setup is used for the experimental mechanical characterization. Numerical and experimental strength analyses are carried out to investigate the effect of the wood's fiber orientation and in-plane loading direction on the joint strength and fracture toughness. The results show that the orientation of the fibers does not affect the tensile and shear strength (2.3 and 7 MPa, respectively). In the case of fracture, the virtual crack closure technique is used in a finite element model to determine the critical values of energy release rate in pure and mixed modes. A mixed mode fracture criterion of the welded joint is determined.

Introduction

Assembling wood is an important issue in structural and furniture applications. Among several solutions available to create a connection between two wood pieces, friction welding has the advantage of being a fast process that does not require the utilization of additional materials. The joint is generated at the interface by a mix of

✉ Martin Rhême
  martin.rheme@bfh.ch

[1] Institute for Material and Wood Technologies, Bern University of Applied Science, Bienne, Switzerland

[2] Laboratory of Applied Mechanics and Reliability Analysis, EPFL, Lausanne, Switzerland

🖄 Springer

molten wood components and wood fibers resulting from the thermo-mechanical effects produced by the friction and then solidified in a holding step (Gfeller et al. 2003; Stamm et al. 2005; Ganne-Chedeville et al. 2006).

The design of wood pieces and structures requires criteria that can be derived from a strength analysis or fracture mechanics. The latter is a convenient tool in the field of wood and welded wood joints, since it takes into account cracks and flaws that naturally occur in this type of material. Welded joints fracture characteristics in pure fracture modes have already been addressed in previous works with double cantilever beam (DCB) and end notched flexure (ENF) specimens (Ganne-Chedeville et al. 2008a; Omrani et al. 2009; Rheme et al. 2013a, b). In real structures, the simultaneous application of tension and shear loads leads to a mixed mode state at the crack front. Moreover, in the case of wood, mode mixity is also induced by the anisotropic properties of the material and is therefore more relevant for real applications.

Several types of specimens, used to test wood and wood joints mixed mode fracture, have been suggested in the literature. Among the most common one can find the mixed mode bending test (MMB) (de Moura et al. 2010, 2011; Yoshihara 2013), the single leg bending, the asymmetrical DCB (Jernkvist 2001) or the asymmetrical wedge splitting (Tschegg et al. 2001). In an early work, Valentin and Caumes (1989) reviewed different kinds of specimens to test pure and mixed modes fracture and suggested the use of a compact tension shear specimen associated with an Arcan device for wood mixed mode fracture investigations. Since then, various studies have used different versions of the Arcan device, which was first developed by Banks-Sills et al. (1983) to test, for example, interfacial and adhesive failure (Choupani 2008; Davies et al. 2009; Golaz et al. 2013; Pang and Seetoh 1997; Rikards 2000) shear properties of wood (Dahl and Malo 2009a, b; Xavier et al. 2009) or fracture properties of wood (Valentin and Caumes 1989; Méité et al. 2013; Franke and Quenneville 2014). In all these works, the authors highlighted the ability of the Arcan test to provide a wide range of mode mixity with the same specimen dimensions simply by rotating the testing device. Recently, Ginest et al. (2012) used the Arcan device to compare the strength values of solid and welded beech, but since no cracked specimens were used in this work, energetic fracture criteria for welded wood joints under mixed mode conditions were not determined.

The influence of the orientation of wood fibers on the shear strength has been reported by Properzi et al. (2005) and Omrani et al. (2010), but opposite conclusions were drawn. The difference between these two studies is mainly the welding parameters, which may explain that in some cases [longer welding time and lower frequency (Properzi et al. 2005)] a difference was observed between parallel- or cross-grain specimens, whereas no differences were apparent in the study by Omrani et al. (2010). However, the testing method could also be questionable, since the wood single lap configuration with a cross-grain specimen induces tensile stresses in the radial direction that are close to the wood strength.

Apart from this, most works dealing with the mechanical characterization of welded wood joints have focused on the case where the fibers of each part are aligned in the same direction. It is, however, of practical interest to characterize the

properties of welded pieces of different fiber orientations (cross-grain), as is the case for cross-laminated wood panels for example.

This work aims to understand the mechanical behavior of welded wood joints. The following topics are investigated: (1) the influence of the wood fiber orientation on the mechanical properties, (2) the isotropy of the mechanical response in the plane of the joint and (3) the characterization of mixed mode fracture behavior. Welded pieces of various fiber orientations are produced by linear friction welding, and specimens are machined from these pieces. A strength analysis is performed in tensile, shear and in mixed mode using an Arcan device to investigate the strengths of the welded joints. FEM is used to design the specimen shape in order to achieve the best homogeneous stress distribution over the welded joints. Fracture investigations are carried out using the same experimental device but with pre-cracked specimens and loaded at various angles in order to induce different mode mixities. FEM associated with virtual crack closure technique (VCCT) is used to separate the energy release rate (ERR) and to determine a criterion for mixed mode fracture of welded wood joints.

Materials and methods

Specimens preparation

Planks of beech wood (*Fagus sylvatica*) are stored in standard climatic conditions (23 °C/55 % relative humidity) until environmental equilibrium moisture content (MC) is achieved. Out of these planks, single wood parts are manufactured to permit the welding of parts with various fiber orientations (Fig. 1a). The orientation of the fibers is carefully selected to always have the tangential direction of the wood in the direction of the thickness, i.e., perpendicular to the welding plane. The other two directions (radial and longitudinal) are varied for each welded piece type (Fig. 1a) and are described according to the angle that the longitudinal direction of each layer makes with the welding oscillation direction (i.e., 0–0, 0–90 and 0–45).

Prior to welding, the planks are planned and cut to the following dimensions:

$$Long : 120 \times 55 \times 10.3 \, mm^3 / Trans : 120 \times 90 \times 10.3 \, mm^3 / Mid$$
$$: 90 \times 90 \times 10.3 \, mm^3$$

The denominations *Long*, *Trans* and *Mid* refer to the specimen cutting in different in-plane directions (Fig. 1b) that serve to distinguish and test the different in-plane direction properties.

All welded pieces are produced by linear friction welding on a Branson M-DT24L welding machine. The welding process is sequenced in two steps. First, the friction step is characterized by a 3 mm amplitude oscillation at 100 Hz for 2.4 s and with a pressure of 1.5 MPa. During the holding step, the same pressure is maintained for 7 s without oscillation.
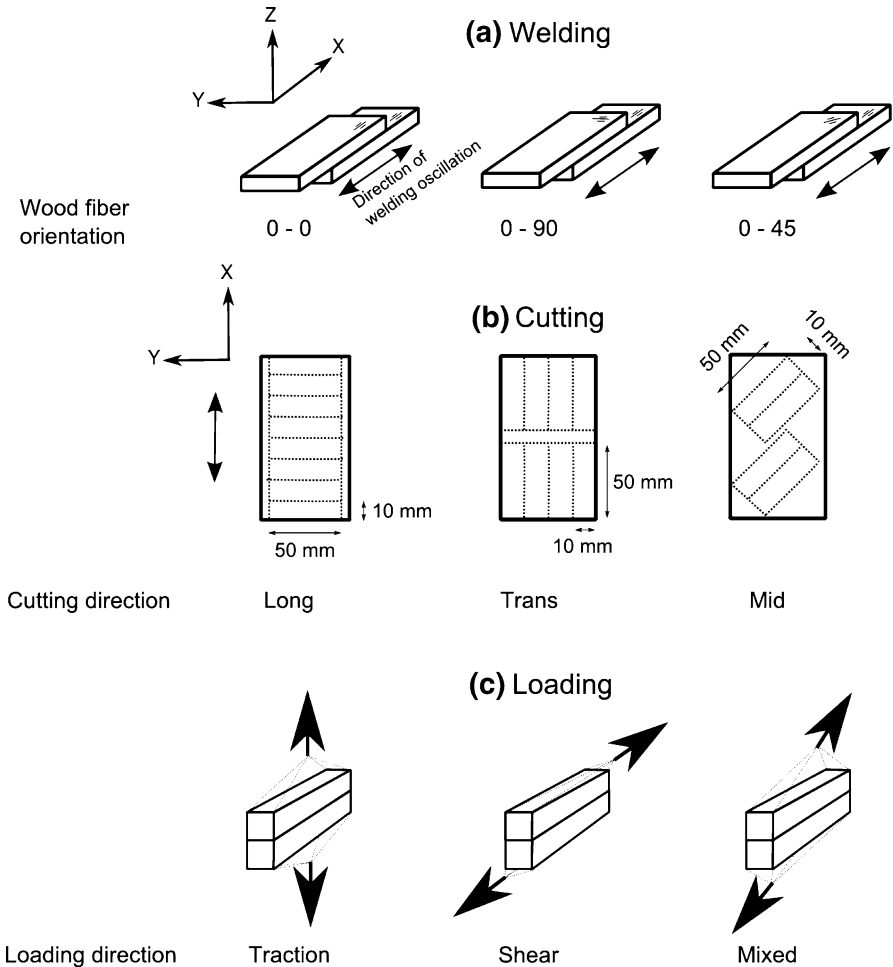
Fig. 1 Schematic presentation of the preparation process and testing of the Arcan specimens. **a** Welding of the wood parts in parallel or cross-grain orientation followed by **b** specimen cutting in the welded piece in different cutting directions in the plane of the weld and finally, **c** mechanical testing with various testing angles

Specimens for strength testing

The Arcan device used in this work imposes the following geometrical limitations on the specimens: the height must be equal to 20 mm, the width smaller or equal to 10 mm and the length smaller or equal to 70 mm. The specimens are initially cut at dimensions of $10 \times 20 \times 50$ mm^3 either perpendicular to the direction of the welding oscillations, parallel to the oscillations or at an angle of 45° (see Fig. 1b). A numerical analysis based on the model presented below is used to determine the optimal dimensions leading to the most homogeneous stress distribution on the joined interface. In addition, practical machining constraints are also taken into account. In particular, numerical studies are
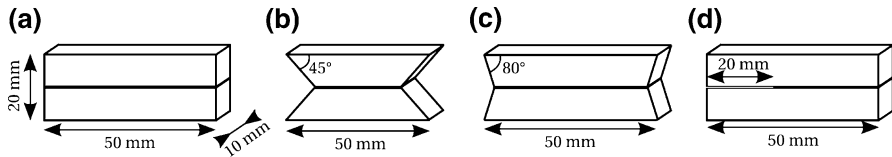
Fig. 2 Dimensions and shapes of the specimens used for the Arcan test in **a** tension, **b** shear, **c** mixed loading and **d** fracture with a 20 mm pre-crack
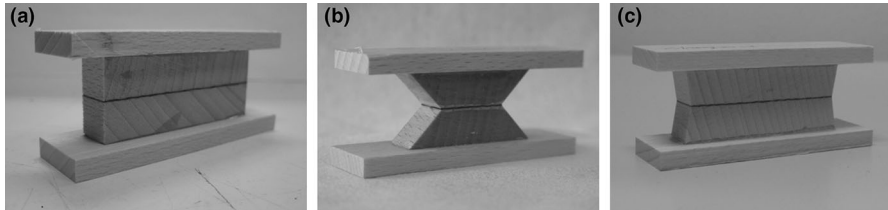

Fig. 3 Examples of specimens before testing for **a** tensile, **b** shear and **c** mixed mode strength

carried out to investigate the effects of edge grooves or variation of length. A detailed explanation of these studies is given in "Specimen design" section. The details of the geometry used for the experimental work are presented in Fig. 2.

The specimens and the necessary edge grooves are cut using a circular saw, and wood support plates are glued with epoxy resin at the top and bottom of each specimen to be inserted in the clamping system of the Arcan device. The final shapes of the specimens are shown in Fig. 3.

Specimens for fracture testing

The geometry of the specimens for all fracture tests (i.e., mode I, mode II and mixed modes) is similar to those used for tensile tests (see previous section). Before gluing the support plates, a band saw of 0.3 mm thickness is used to cut a notch from one edge of the specimen, along the joined interface and over a distance of 19.5 mm. To initiate the crack in the joining material, the notch is further increased with the help of a razor blade until it reaches ~ 20 mm and the length is precisely measured with a binocular magnifier. For the fracture testing, only parallel (0–0) and cross-grain (0–90) specimens with the *Trans* cutting direction are produced.

Experimental methods

Arcan testing

The Arcan testing device is presented in Fig. 4. The orientation of the device can be varied to reach different loading angles with respect to the weld plane. Shear is achieved with a 0° loading angle and tension with 90° (mode II and mode I for the cracked specimens, respectively). In between, mixed modes are possible with various angles of 15° steps. The same device is used for the strength analysis (with
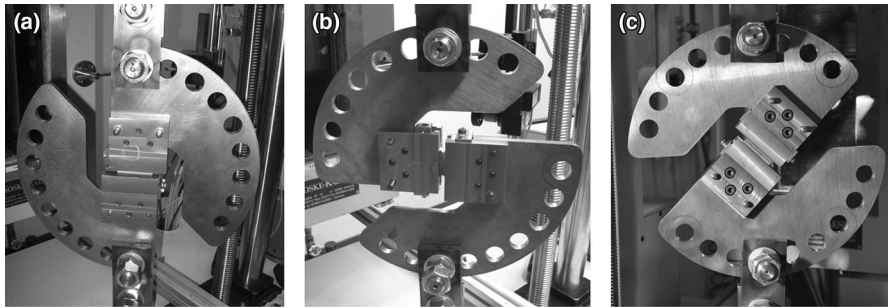
Fig. 4 Photograph of the Arcan setup positioned for **a** tensile testing, **b** shear testing and **c** mixed mode testing at an angle of 45°

loading angles 0°, 45° and 90°) and for the fracture analysis (with loading angles of 0°, 15°, 30°, 45° and 90°). For each kind of test and each combination of angles and fiber orientation, 5 specimens are tested.

Finite element model

Before manufacturing the specimens, parametric studies are performed using a numerical model to investigate the effect of the specimens' geometry on the stress distribution on the joined interface.

A 3D model is built using Dassault Simulia Abaqus/CAE software. This model consists of two 3D deformable parts representing the two adherents of the joint. Each part has its own cylindrical coordinate system that serves as reference for the material orientation. The origin of the coordinate system is situated at a distance of 300 mm from the center of the part to represent the actual year ring orientation (Fig. 5b). The Arcan device is modeled according to its real dimensions, but its gripping system is simplified and modeled as a rigid steel block onto which the specimen is attached with a tie constraint (Fig. 5a). Each part of the Arcan device is composed of 2693 C3D4 elements.

The material properties are considered orthotropic linear elastic and similar to the properties defined in Rheme et al. (2013a, b). The properties are considered MC dependent, but in this work, MC of the tested parts is kept constant at 11.8 % (measured by the oven drying method).

For the strength analysis, the interest lies in the investigation of the stresses distribution over the welded interface. Hence, to simplify the model, it is assumed that the joint perfectly transmits degrees of freedom (DOE) to both wood pieces and is modeled with a tie constraint. The two parts of the specimens are meshed with 5104, 3776 and 5824 linear 3D stress hexahedral elements (C3D8R) for the tensile, shear and mixed loading, respectively. Since the interest lies in the investigation of the portion of the surface where the normalized stresses are uniform and to avoid high computation time issues, no mesh refinement at the edge is carried out. The load is applied at a reference point situated at the center of the loading hole of the Arcan device, which in turn is linked to the internal surface of the hole by a multiple
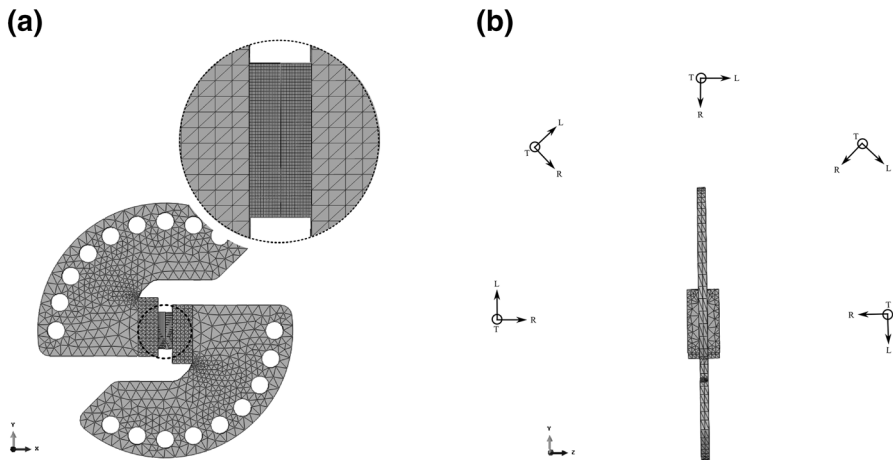
Fig. 5 **a** *Front view* of the FE model representing the Arcan device and magnification of a specimen for VVCT. **b** *Side view* with the various coordinate systems for material orientation. The global coordinate systems are located at the *bottom* left part of part **a** and **b** of the figure

point constraint (MPC). Furthermore, the displacement of this control point is limited to the direction of loading. The opposite reference point is similarly linked to the device and constrained by a pin boundary condition.

For fracture analysis, a master–slave contact pair is defined as bonded in the initial conditions, leaving a 20 mm pre-crack on one side. In order to use VCCT to calculate mode mixity, the debonding is enabled in the loading step with a VCCT energy-based crack propagation criterion with a power law mixed mode behavior. Since only mode mixity and static cases are of interest here and the model is linear, all the critical energy release rate ERR values and the mixed mode parameters are set to unity to avoid crack propagation.

In the case of the fracture analysis, the mesh size in the direction normal to the joint plane is set to 0.5 and 5 mm in the direction of the crack propagation based on a mesh convergence study. This leads to a specimen containing 4800 C3D8R elements. It should be noted that the values of energy release rate ERR converge when decreasing the element height, but comparatively long element lengths are needed to avoid the effect of oscillating stresses and ERR near the crack front, which is a limitation of the VCCT method (Krueger 2004).

Results and discussion

Strength analysis

Specimen design

In order to evaluate the stress distribution on the interface between the wood pieces and show the effect of different types of grooves, the shear and tensile stresses on a
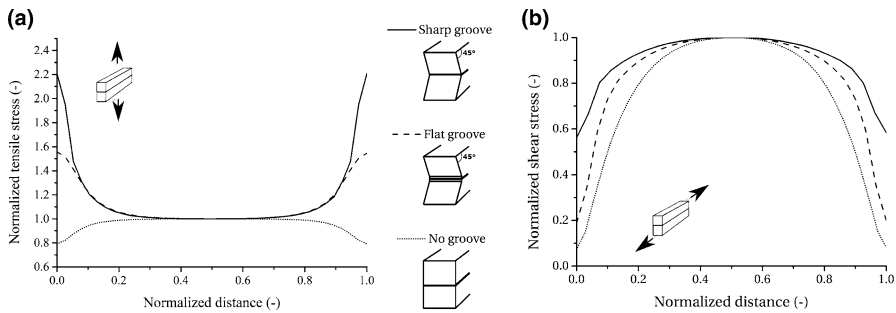
Fig. 6 **a** Distribution of tensile stress along the interface during tensile test and **b** distribution of shear stress during shear test. Both graphics show the influence of grooves cut into the edges of the specimens. "Sharp" and "Flat" refer to the shape of the bottom of the groove at the level of the joint

path running along the length of the specimen in the middle of the surface are calculated using the FE model. Figure 6 shows the influence of a selection of groove geometries on normal and shear stress distribution in the joint. It must be noted that because the mesh is not specially refined at the edge, artifacts and not accurate solutions can appear in the region of the graph near the 0 and 1 normalized distance. The stress values are all normalized to the value in the middle of the profile and, since the length of the joint varies with the type of groove, the distances are also normalized in this graph. In the case of shear testing, it has been found that the optimal solution is a sharp groove with a 45° angle; however, it is more advantageous to avoid using any groove for the tensile test.

When the grain orientation is not in the load direction, attention must be paid to the stress distribution, not only on the welded interface, but also in the wood. This is the case, for example, for the 0–0 *Long* specimens loaded in pure shear where failure in the wood and in the joint are observed. Numerical analysis shows that under these conditions high shears and tangential tensile stresses develop in the bulk of the wood near the free edges. The values of tangential tensile stresses (5.4 MPa) given by the FEM are close to the strength reported by Ozyhar et al. (2012) and could lead to bulk failure in the wood. Attempts to experimentally discriminate between failure initiation in the wood or in the joint were not successful, even with the help of a high-speed camera during the test (6000 frames per second). After several trials, it proved impossible to design a specimen shape where both tangential tensile stress and shear stress concentrations are sufficiently reduced. Finally, to circumvent this issue in this specific case only, wood surface of the specimens is covered with a thin layer of epoxy resin, which is just sufficient to avoid crack initiation on the free edges of the wood block.

Figure 7 shows the influence of the angle of the groove on both the tensile and shear stress distributions along the interface for a loading angle of 45°. In this case, a groove with an angle of 80° is chosen as the best compromise between shear and tensile stress uniformity. Since the profiles of stresses are considered sufficiently homogeneous in the optimized configurations, especially in the shear loading, the
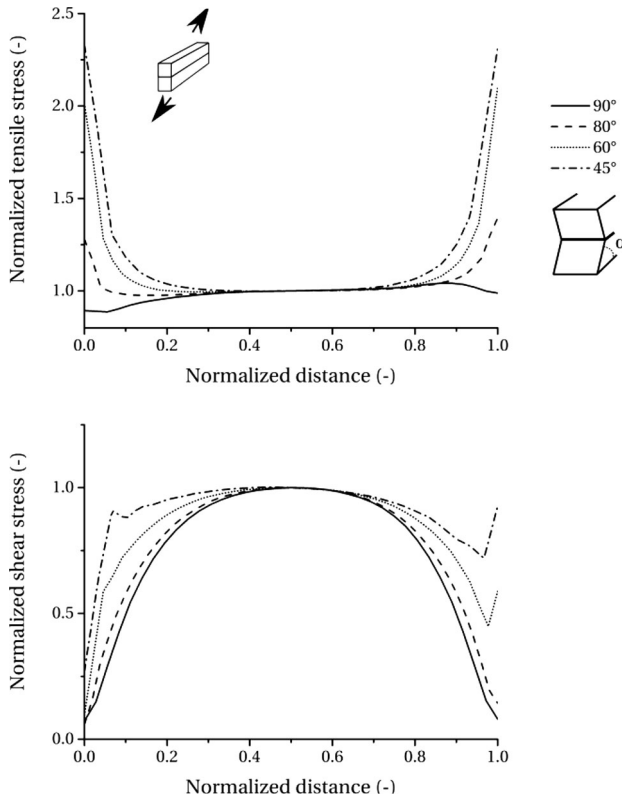
Fig. 7 Effect of the groove's cutting angle on the tensile (*top*) and shear (*bottom*) stress distribution with a mixed loading (45° loading angle)

strengths of the joint will be subsequently computed as the ratio of the experimental failure load over the tested area (average nominal stress).

As specified in "Specimens preparation" section, the ideal angle of the year ring with the joint interface is 90°. In practice, this condition is not always simple to achieve for each specimen, but numerical analysis has shown that for all loading angles, a deviation of this angle up to 45°, which is an extreme case, does not induce more than a 1.8 % variation of the stresses on the joint. It is therefore assumed that the year ring angle is constant and equal to 90° even if small variations are present on the specimens.

Mechanical strength

The measured values of strengths, i.e., failure load divided by joined surface, for each group of specimens and for three different loading angles are presented in Fig. 8. Each bar on the graphs represents the average of 5 tested specimens. Although there is scatter in certain orientations and loading conditions, an analysis of variance (ANOVA) of all the data confirms that neither the in-plane direction
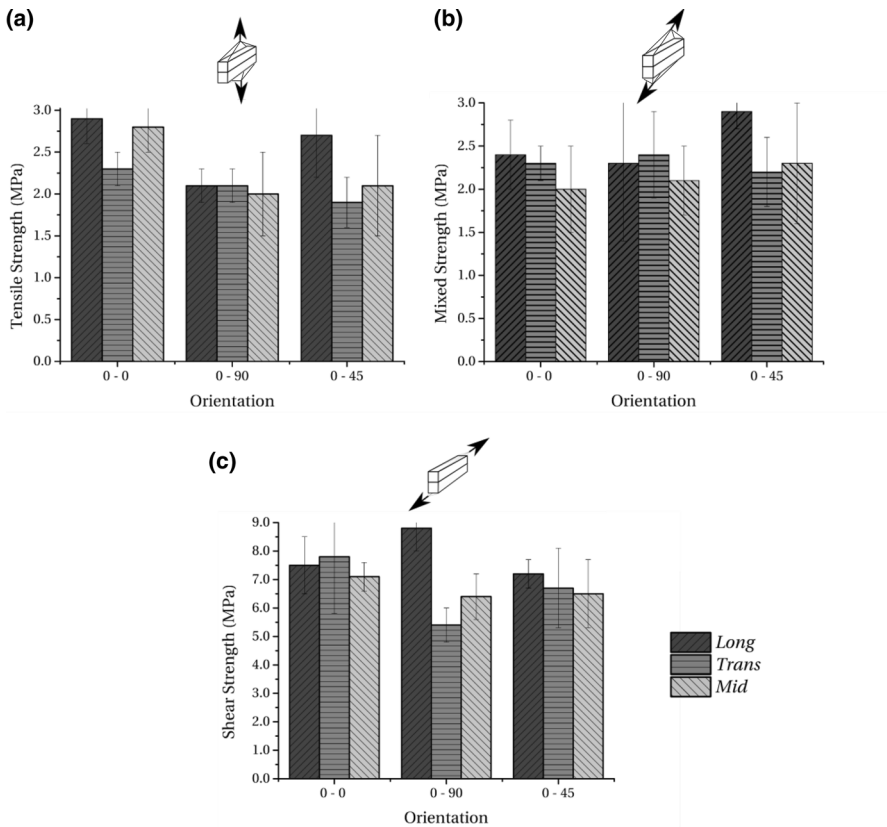
(a)

(b)

(c)

Fig. 8 Tensile (**a**), mixed (**b**) and shear (**c**) strength (i.e., average nominal stresses at failure during testing in tension, with 45° angle loading and in shear, respectively) measured with the Arcan test

(*Long*, *Trans* and *Mid*) nor the plies' orientation (0–0, 0–45 and 0–90) have an influence on the strength of the welded joint. No statistical difference is observed, and the null hypothesis H_0 is accepted with a *p* value equal to 0.15, 0.81 and 0.96 for tensile, shear and mixed loading, respectively.

The present results show that the strength properties of the joining material can be considered transversely isotropic and that the orientation of the wood fibers during the welding is not a parameter that has a strong influence on the strength properties of the joining material. Indeed, as revealed by microscopical observations presented in Fig. 9, the joining material is composed of a random distribution of wood fibers embedded in a matrix material where no preferential orientation is observed. It seems that the welding process cancels the anisotropy of the wood by creating a layer of a new transversely isotropic composite material, whose properties are subsequently not influenced by the orientation of the surrounding wood fibers. Consequently, the strength value can be calculated for each loading angle by averaging the values of all corresponding groups in tensile, mixed and shear loading. This results in strength equal to 2.3, 2.3 and 7 MPa in tensile, mixed
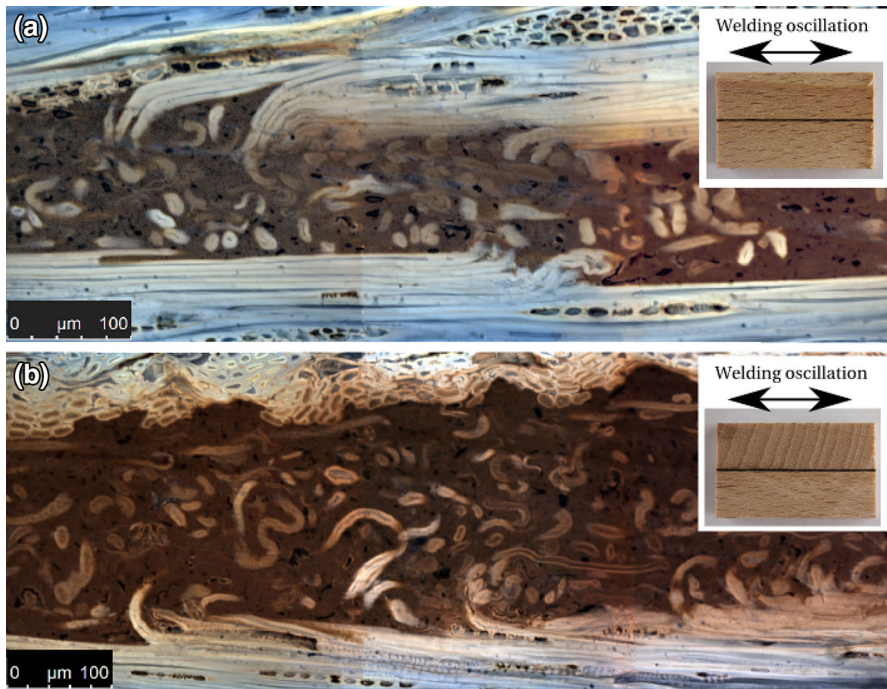
Fig. 9 Side view of the **a** 0–0 and **b** 0–90 specimens taken with confocal autofluorescence microscopy and optical photography (*box*). The wood fibers are either *blue* or *yellowish*, and the joining material is the *brown part* in the center of the images (see color figure in online publication)

and shear loadings, respectively. The mixed mode strength value is very close to the tensile strength and seems to indicate that, although the 45° loading angle generates a mixed tensile and shear stress state at the joined interface, the specimens fail due to tensile dominated strength.

The strength values determined by Ginest et al. (2012) with uncracked welded beech specimens (1.73 and 4.64 MPa for tensile and shear strength, respectively) are closer to the pure mode values from the notched specimens of this work ("Fracture analysis" section) than the strength values. The shape of the mixed mode loading strengths envelop is also very different. In this work, the welding parameters, the Arcan device and the specimens' dimensions are different to those used by Ginest et al. (2012) and no direct comparison is therefore possible, but it shows that production parameters and testing conditions have a strong influence on the results. However, the strength properties measured in this study are consistent with the results of Ganne-Chedeville et al. (2008b) who measured shear strength with a tensile shear test of about 8 MPa for beech welded under similar frequency, time and MC conditions. Rheme et al. (2013a, b) have also measured similar strength values in tension and shear, respectively. Interestingly, these strength levels are lower than the wood strength and comparable with polymeric foam (Ashby 2011).

Fracture analysis

The VCCT enables computing and separating the ERR corresponding to mode I and mode II loading at the crack front. Figure 10 shows examples of ERR values along the crack front for different loading angles corresponding to the experimentally tested ones (0°, 15°, 30°, 45° and 90°). Except for some limited edge effects, the
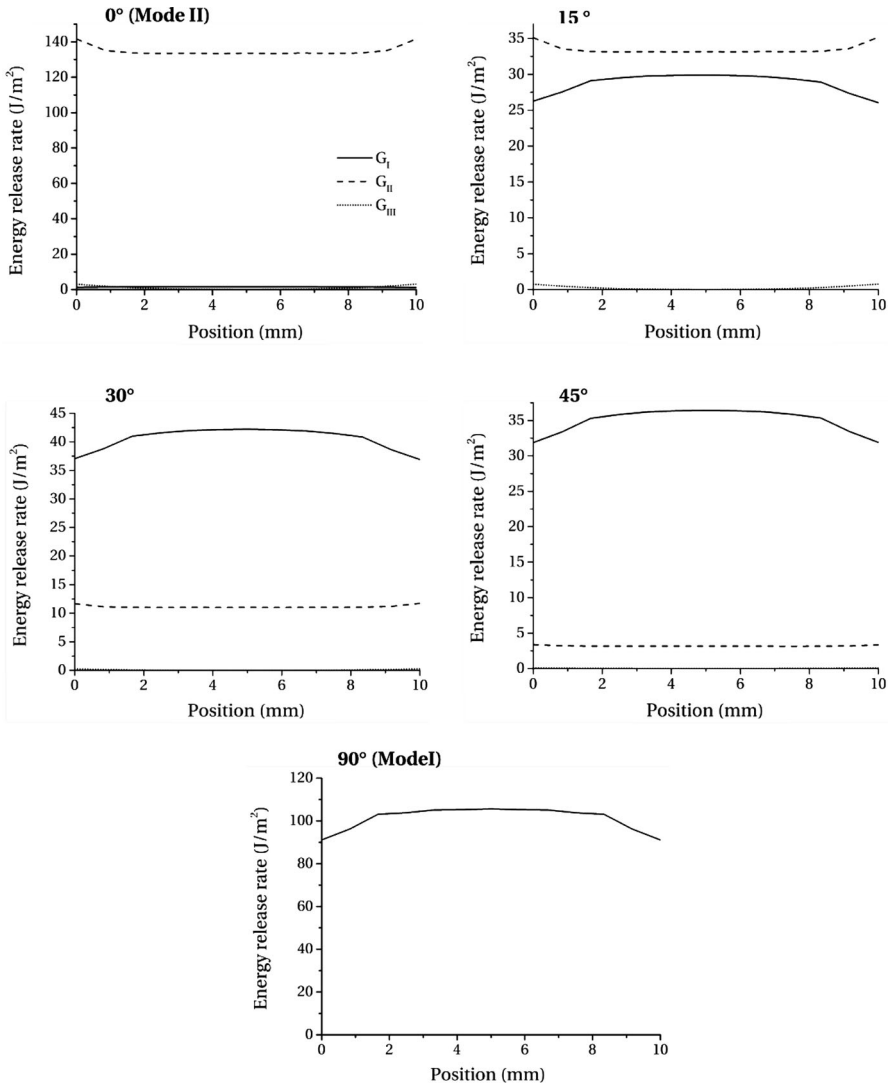

Fig. 10 Examples of ERR profiles along the crack front determined by FEM with VCCT for each loading angle tested in the experimental part. The loads used in the model are the average of the experimental maximal loads of the 0–0 specimens, and the values are measured at the nodes situated at the crack front

values of ERR are constant all along the crack front. This numerical analysis enables verifying that the experimental setup gives a well-determined pure mode I or pure mode II when loaded at 90° and 0°, respectively, as only G_I or G_{II} values are significant in those cases. It is revealed that mixed modes seem to occur only when the loading angle is between 0° and 45°, an angle at which the mixed mode ratio G_{II}/G_{tot} is already as low as 0.08. When loading angles are higher than 45°, the applied nominal mode I is even more important. Its experimental value, however, is partially influenced by the experimental setup (experimental device, specimen geometry, etc.) and the material properties. This explains why the 0–0 and 0–90 specimens have slightly different mixed mode ratios at the same loading angle.

The experimental load–displacement curves obtained with the Arcan test and the pre-cracked specimens show that unstable crack propagation occurs once the initiation conditions are fulfilled. Therefore, for each specimen, the experimental load at failure is taken as a critical value and is inserted in the numerical model as a loading condition, and the calculated ERRs are considered as the critical ERR values. The values of G_{III} are considered negligible and are therefore not reported hereafter. Figure 11 shows the graphs of the values of G_I and G_{II} for all specimens. Graphs (a) and (b) present the results for one of the two different types of fiber orientation, 0–0 and 0–90, respectively. The scatter is mostly due to heterogeneity of the wood and joining material. It is interesting to mention that, in both types of orientation, the introduction of a small amount of mode mixity leads to a drastic drop of the fracture energy, which is even more pronounced for the 0–0 specimens. The critical ERRs in pure modes are similar for both welding orientations, but the 0–90 welding orientation seems to have slightly better resistance in the mixed mode. The trend of the data showing that critical ERRs are smaller in the mixed modes than in pure modes has already been reported by Tschegg et al. (2001) for wood and Singh et al. (2010) for wood adhesive.
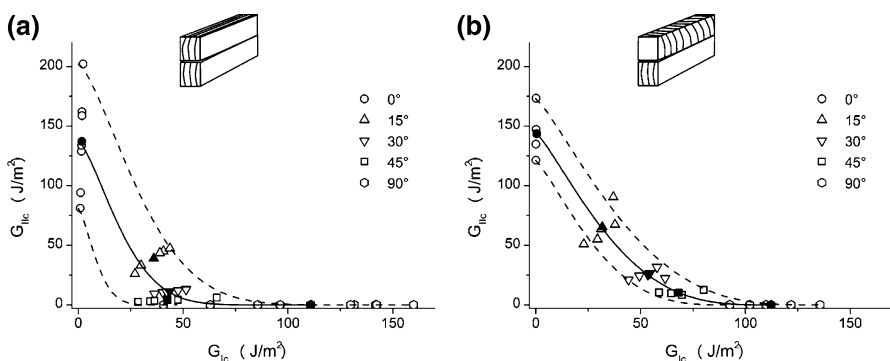

Fig. 11 Critical ERR values determined with combined Arcan experiment and VCCT, **a** for the 0–0 specimens and **b** for the 0–90. The *empty symbols* are the individual critical ERR values for each specimen. The *filled symbols* show the average value of each group of specimens tested with the same loading angle. The *solid lines* are drawn according to Eq. (1) and the parameters determined with the average values. The *dashed lines* represent the extreme values (see text)

The following power expression is used to express the fracture criterion (Valentin et al. 1991; Reeder 2006).

$$\left(\frac{G_I}{G_{Ic}}\right)^n + \left(\frac{G_{II}}{G_{IIc}}\right)^m = 1 \tag{1}$$

The critical values G_{Ic} and G_{IIc} are computed from the average of the specimens tested with a loading angle of 90° and 0°, respectively, while the parameters n and m are determined with a least square fitting of the experimental data. For both specimens type (0–0/0–90), the identification procedure leads to the following values: $G_{Ic} = 110/112$ (J/m^2), $G_{IIc} = 137/144$ (J/m^2), $n = 1.43/1.22$ and $m = 0.12/0.30$. With this analysis, a mixed mode fracture envelop is determined, as presented in Fig. 11 (solid lines) and shows a concave shape, highlighting the high sensitivity of the welded joint to mixed mode loading. By keeping the n and m parameters and using the maximal and minimal values of the pure modes as G_{Ic} and G_{IIc}, one can draw a zone, marked out with dashed lines in Fig. 11, that encompasses all the experimental data, hence separating a safe and critical region where failure is unlikely or certain to occur. The fact that this zone is narrower for the 0–90 specimens is mostly due to the smaller scatter of the result in the pure mode. Nevertheless, a better understanding of this complex mixed mode behavior should be achieved through a micromechanics analysis; however, this is not the aim of this study. In particular, the effect of mode mixity on the crack path within the joining material and on any fiber pullout should be investigated, taking into account the heterogeneous nature of the joining material. Indeed, at the microscale, the joining material is a mixture of voids, modified wood components matrix and wood fibers rendering the material response nonlinear. Therefore the observed behavior could be caused by the development of sub-critical local damage, or a plasticity region in the joining material around the crack tip, which could blunt and delay crack propagation in the pure mode cases. Although the exact causes for such behavior are for the moment unknown, the comparison of the Arcan test from the present study with the values determined in other works (Rheme et al. 2013a, b, 2014) with DCB, ENF and MMB tests shows a good correlation and suggests that the fracture energies are correctly determined by the Arcan test (Fig. 12).

Fig. 12 Fracture envelop for 0–0 welding orientation compared with the results of ENF, MMB and DCB test. *Solid* and *dashed lines* are drawn according to Eq. (1) and results of the Arcan test (see text and Fig. 11)
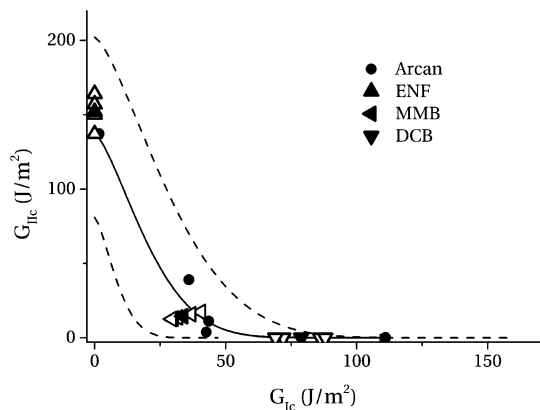
Equations (2) and (3) are used to compute the nominal tensile and shear stresses occurring at the bonded part of the cracked specimens at the time of failure. F is the average maximal load for each loading angle, S is the bonded area, and α is the angle of loading.

$$\sigma_y = \frac{F}{S}\cos(\alpha) \tag{2}$$

$$\tau_{xy} = \frac{F}{S}\sin(\alpha) \tag{3}$$

When one looks at the $\sigma_y - \tau_{xy}$ values pairs for each loading orientation, it is observed that the nominal stress values do not differ substantially between uncracked and pre-cracked specimens. This indicates that, within the approximations of the analysis on the stress distributions on the joints, the failure of the pre-cracked specimen is not driven by the fracture mechanics but by stress-driven failure initiation. Indeed, the strength properties of the joining material are sufficiently low so that no significant stress concentration occurs at the pre-crack tip and therefore does not play an important role. Consequently, the ERR determined in this work might not be interpreted as material properties but depend on the test and specimens geometry.

Conclusion

The strength and fracture properties of welded wood joints were investigated by a coupled experimental and numerical work. The Arcan device was a convenient tool to investigate the effect of mixed mode loading of wood pieces welded in the parallel or cross-grain fiber direction. The tensile strength of the welded joint was found to be at 2.3 MPa and the shear strength at 7 MPa. Both properties have shown to be statistically independent of the fiber orientation in the welded wood layers in relation to the direction of the welding oscillation. Furthermore, the shear strength was found to be independent of the shear direction in relation to the different fiber orientation combinations of the welded wood layers.

The experimental tests with pre-cracked specimens produced unstable crack propagation and sudden failure. The maximal experimental loads inserted in the FE model enabled computing and separating the ERRs. Parameters for a mixed mode power fracture criterion were determined and showed a concave fracture envelop with lower critical ERR values in the mixed modes than in the pure modes. However, the ERR values must be taken with caution since they might not be totally independent from the test and specimens geometry.

References

Ashby MF (2011) Materials selection in mechanical design. Elsevier, Amsterdam

Banks-Sills L, Arcan M, Bui H (1983) Toward a pure shear specimen for K_{IIc} determination. Int J Fract 22:R9–R14

Choupani N (2008) Interfacial mixed-mode fracture characterization of adhesively bonded joints. Int J Adhes Adhes 20:267–282

Dahl K, Malo K (2009a) Linear shear properties of spruce softwood. Wood Sci Technol 43:499–525

Dahl K, Malo K (2009b) Nonlinear shear properties of spruce softwood: numerical analyses of experimental results. Compos Sci Technol 69:2144–2151

Davies P, Sohier L, Cognard JY, Bourmaud A, Choqueuse D, Rinnert E, Créac'hcadec R (2009) Influence of adhesive bond line thickness on joint strength. Int J Adhes Adhes 29:724–736

de Moura M, Oliveira J, Morais J, Xavier J (2010) Mixed-mode I–II wood fracture characterization using the mixed-mode bending test. Eng Fract Mech 77:144–152

de Moura M, Oliveira J, Morais J, Dourado N (2011) Mixed-mode (I + II) fracture characterization of wood bonded joints. Constr Build Mater 25:1956–1962

Franke B, Quenneville P (2014) Analysis of the fracture behavior of Radiata Pine timber and laminated veneer lumber. Eng Fract Mech 116:1–12

Ganne-Chedeville C, Properzi M, Pizzi A, Leban J, Pichelin F (2006) Parameters of wood welding: a study with infrared thermography. Holzforschung 60:434–438

Ganne-Chedeville C, Duchanois G, Pizzi A, Pichelin F, Properzi M, Leban J (2008a) Wood welded connection: energy release rate measurement. J Adhes Sci Technol 22:169–179

Ganne-Chedeville C, Properzi M, Leban JM, Pizzi A, Pichelin F (2008b) Wood welding: chemical and physical changes according to the welding time. J Adhes Sci Technol 22:761–773

Gfeller B, Zanetti M, Properzi M, Pizzi A, Pichelin F, Lehmann M, Delmotte L (2003) Wood bonding by vibrational welding. J Adhes Sci Technol 17:1573–1589

Ginest B, Cognard JY, Pizzi A (2012) Analysis of the mechanical behavior of wood and welded wood under tensile-shear loads using a modified Arcan device. J Adhes Sci Technol 26:1717–1731

Golaz B, Michaud V, Lavanchy S, Manson JA (2013) Design and durability of titanium adhesive joints for marine applications. Int J Adhes Adhes 45:150–157

Jernkvist L (2001) Fracture of wood under mixed mode loading II. Experimental investigation of picea abies. Eng Fract Mech 68:565–576

Krueger R (2004) Virtual crack closure technique: history, approach and applications. Appl Mech Rev 57(2):109–143

Méité M, Dubois F, Pop O, Absi J (2013) Mixed mode fracture properties characterization for wood by digital images correlation and finite element method coupling. Eng Fract Mech 105:86–100

Omrani P, Mansouri H, Duchanois G, Pizzi A (2009) Fracture mechanics of linearly welded wood joints: effect of wood species and grain orientation. J Adhes Sci Technol 23:2057–2072

Omrani P, Mansouri H, Pizzi A, Masson E (2010) Influence of grain direction and pre-heating on linear wood welding. Eur J Wood Prod 68:113–114

Ozyhar T, Hering S, Niemz P (2012) Moisture dependent elastic and strength anisotropy of european beech wood in tension. J Mater Sci 47:6141–6150

Pang H, Seetoh W (1997) A compact mixed mode (CMM) fracture specimen for adhesive bonded joints. Eng Fract Mech 57:57–65

Properzi M, Leban J, Pizzi A, Wieland S, Pichelin F, Lehmann M (2005) Influence of grain direction in vibrational wood welding. Holzforschung 59:23–27

Reeder JR (2006) 3d Mixed-mode delamination fracture criteria—an experimentalist's perspective. In: American Society for composites 21st annual technical conference

Rheme M, Botsis J, Cugnoni J, Navi P (2013a) Influence of the moisture content on the fracture characteristics of welded wood joint—part 1: mode I fracture. Holzforschung 67:747–754

Rheme M, Botsis J, Cugnoni J, Navi P (2013b) Influence of the moisture content on the fracture characteristics of welded wood joint—part 2: mode II fracture. Holzforschung 67:755–761

Rheme M, Botsis J, Cugnoni J, Parviz N (2014) Mixed mode crack propagation in welded wood joint. Eng Fract Mech, Submitted

Rikards R (2000) Interlaminar fracture behaviour of laminated composites. Comput Struct 76:11–18

Singh HK, Chakraborty A, Frazier CE, Dillard A (2010) Mixed mode fracture testing of adhesively bonded wood specimens using a dual actuator load frame. Holzforschung 64:353–361

Stamm B, Natterer J, Navi P (2005) Joining wood by friction welding. Holz Roh Werkst 63:313–320

Tschegg E, Reiterer A, Pleschberger T, Stanzl-Tschegg S (2001) Mixed mode fracture energy of sprucewood. J Mater Sci 36:3531–3537

Valentin G, Caumes P (1989) Crack propagation in mixed mode in wood: a new specimen. Wood Sci Technol 23:43–53

Valentin GH, Boström L, Gustafsson P, Ranta-Maunus A, Gowda S (1991) Application of fracture mechanics to timber structure rilem state-of-the-art report. Technical Report 1262, Technical Research Center of Finland

Xavier J, Oliveira M, Morais J, Pinto J (2009) Measurement of the shear properties of clear wood by the Arcan test. Holzforschung 63:217–225

Yoshihara H (2013) Initiation and propagation fracture toughness of solid wood under the mixed mode I–II condition examined by mixed-mode bending test. Eng Fract Mech 104:1–15